

Comparison of Die Level Stresses in Chip-on-Board Packages Processed with Convection and Variable Frequency Microwave Encapsulant Curing

Yida Zou
R. Wayne Johnson
Jeffrey C. Suhling
Richard C. Jaeger
ME and EE Depts.
Auburn University
200 Broun Hall
Auburn, AL 36849
Phone: 334-844-1880

Email: johnson@eng.auburn.edu

Joe Harris
Cheryl Kromis
Nextek, Inc.
201 Next Technology Dr.
Madison, AL 35728
Phone: 256-722-0400

Iftikhar Ahmad
Denise Tucker
Zak Fathi
Lambda Technologies
860 Aviation Parkway
Suite 900
Morrisville, NC 27560
Phone: 919- 462-1919

Abstract

Liquid encapsulation is used to provide protection to semiconductor die and wires in Chip-on-Board (COB) applications. The cure time for the encapsulant is typically 1.5 to 7 hours with convection curing. The longer convection cure times are often specified to reduce stress and warpage. Such long cure schedules negatively impact manufacturing cycle times and work-in-process. They also delay process feedback. The use of Variable Frequency Microwave (VFM) curing systems has been shown to significantly reduce the encapsulant curing time (35 minute soak). In this work, the impact of VFM curing on the stresses at the die surface has been examined. Stress in the silicon die can produce parameter shifts in analog and mixed signal devices. In addition, stress at the die-encapsulant interface can also lead to delamination during thermal cycling or shock. This in turn can allow moisture ingress and corrosion, or result in shearing of wire bonds during continued thermal cycling.

Using special (111) oriented silicon stress test chips, the die surface stress due to encapsulation was measured for a commercial liquid encapsulant material processed with both convection and VFM curing. The test die had dimensions of 1.02 cm x 1.02 cm, and contained an array of optimized eight-element dual polarity piezoresistive sensor rosettes that are uniquely capable of evaluating the complete stress state (6 stress components) at points on the surface of the die. Stresses were monitored in-situ during the convection cure cycle. However, microwave interference with the measurement signals did not permit in-situ monitoring for the VFM cure. A comparison was made between the room temperature stresses found with each method of curing. After cure, the samples from each curing method were divided into two groups, and reliability tests were performed. The first group of samples was subjected to thermal cycling between -40°C and $+125^{\circ}\text{C}$. The second group was exposed to high humidity storage at 85% RH and 85°C . In each case, changes in the die stress levels were monitored for samples from each curing method to detect delaminations due to thermal cycling and to study the impact of moisture absorption. Finally, a comparison of the stresses introduced at the FR-4 board level for each curing method was made through substrate warpage measurements. VFM curing was found to offer similar die stress levels and reliability, reduction in substrate warpage, and greatly reduced cure times when compared to conventional convection curing.

Key Words: Chip-on-Board, Encapsulant, Variable Frequency Microwave Curing

Introduction

Liquid encapsulation of semiconductor devices continues to grow in both single chip and chip-on-board (COB) assembly. The industry trends of larger die and thinner laminates pose challenges to encapsulation. Increasing die sizes lead to increased

stresses at the die-to-encapsulant interface, while thinner laminates result in increased substrate warpage. Excessive die stresses can result in delamination or fracture of the silicon die. Warpage leads to problems at the next level of assembly.

To address stress and warpage issues, new generations of liquid encapsulants are being

formulated which have low shrinkage during curing and low coefficients of thermal expansion (CTE). In addition, longer cure cycles are being recommended to minimize warpage. Such longer cure times (typically 5-7 hours) translate to more work-in-progress, longer cycle times, and delays in process feedback.

Variable frequency microwave (VFM) processing has been developed as an alternative to convection curing. In recent work, VFM techniques have been shown to significantly reduce epoxy curing times [1,2]. In this paper, die level stresses and substrate warpages are compared for COB packages processed using convection and VFM curing.

Using special (111) oriented silicon stress test chips, the die surface stress due to encapsulation was measured for a commercial encapsulant cured with both convection and VFM curing. The test die contained an array of optimized sensor rosettes that are capable of evaluating the complete stress at points on the surface of the die. Stresses were monitored in-situ during the convection cure cycle. However, microwave interference with the measurement signals did not permit in-situ monitoring for the VFM cure. A comparison was made between the room temperature stresses found with each method of curing. After cure, the samples from each curing method were divided into two groups, and reliability tests were performed. The first group of samples was subjected to thermal cycling over the range of $-40\text{ }^{\circ}\text{C}$ and $+125\text{ }^{\circ}\text{C}$. The second group was exposed to high humidity storage at 85% RH and $85\text{ }^{\circ}\text{C}$. In each case, changes in the die stress levels were monitored for samples from each curing method to detect delaminations due to thermal cycling and to study the impact of moisture absorption. Finally, a comparison of the stresses introduced at the FR-4 board level for each curing method was made through substrate warpage measurements.

Piezoresistive Sensors

Piezoresistive stress sensors are a powerful tool for experimental structural analysis of electronic packages. Figure 1 illustrates the basic application concepts. The structures of interest are semiconductor (e.g. silicon) chips that are incorporated into electronic packages. The sensors are resistors, which are conveniently fabricated into the surface of the die using current microelectronic technology. The sensors are not mounted on the chips. Rather, they are an integral part of the structure (chip) to be analyzed by the way of the fabrication process.

The stresses in the chip produce resistance changes in the sensors (due to the piezoresistive effect) which can be measured. Therefore, the sensors are capable of

providing non-intrusive measurements of surface stress states on a chip even within encapsulated packages. If the piezoresistive sensors are calibrated over a wide temperature range, thermally induced stresses can be measured. Finally, a full-field mapping of the stress distribution over the surface of a die can be obtained using specially designed test chips that incorporate an array of sensor rosettes. A comprehensive review of piezoresistive sensor issues has been given by Sweet [3].

Theoretical analysis has established that properly designed sensor rosettes on the (111) silicon wafer plane can be used to measure the complete state of stress (six stress components) at a point on the top surface of the die [4-6]. Four of the six stress components can be evaluated in a temperature compensated manner. In previous studies, the authors have demonstrated the application (111) silicon test chips for die stress characterization in molded quad flat packs (QFP's) [7] and COB packages (convection cured) [8]. In the prior COB study, in-situ stress measurement during encapsulant cure was first demonstrated.

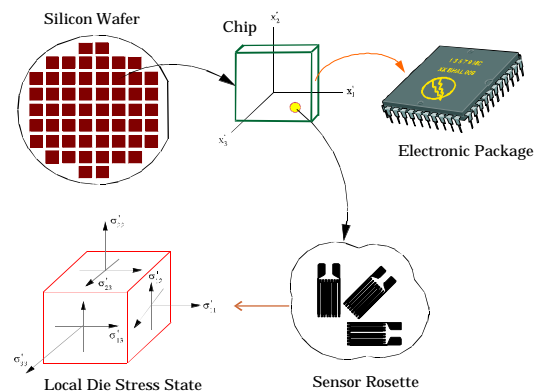


Figure 1 - Piezoresistive Sensor Concept

BMW2 (111) Silicon Test Chip

For packaging studies, (111) silicon test chips (BMW-2) have been fabricated that incorporate an array of optimized stress measurement rosettes and contain perimeter pads suitable for wire bonding. A schematic of the basic die image (200 x 200 mils or 5.1 x 5.1 mm) is shown in Figure 2. A diagram of the optimized eight-element dual polarity sensor rosette is shown in Figure 3. The eight rosette elements are routed to the die bond pads in a manner that allows them to be configured as four two-element half-bridges in order to simplify the resistor change measurements. A fully ion-implanted process has been used to balance the n- and p-type sheet resistances and resistor values, while

maintaining high sensitivity to stress. Process simulations and experimental calibration results from a processing matrix have verified that relatively large values of the piezoresistive coefficients have been achieved.

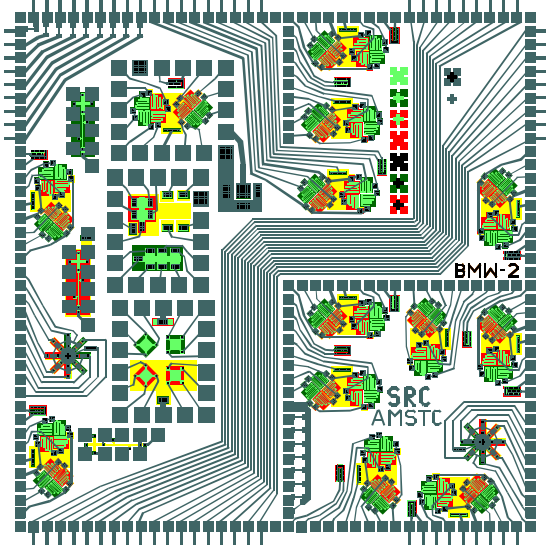


Figure 2 – (111) Silicon BMW-2 Stress Test Chip

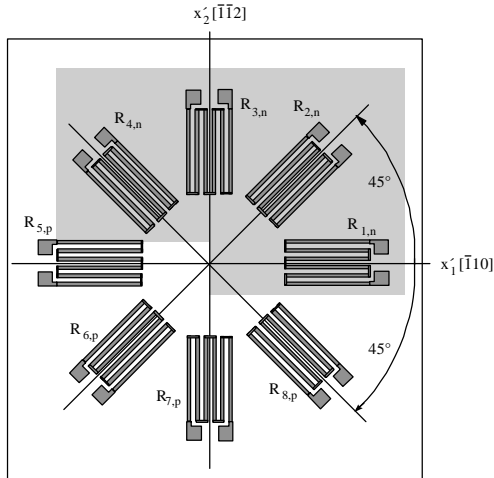


Figure 3 - Optimized Eight Element Sensor Rosette on (111) Silicon

For the rosette in Figure 3, the appropriate expressions for the temperature compensated stress components are [4-6]:

$$\begin{aligned} \sigma'_{11} - \sigma'_{22} &= \frac{(B_3^p - B_2^p) \left[\frac{\Delta R_1}{R_1} - \frac{\Delta R_3}{R_3} \right] - (B_3^n - B_2^n) \left[\frac{\Delta R_5}{R_5} - \frac{\Delta R_7}{R_7} \right]}{[(B_2^p - B_1^p) B_3^p + (B_1^p - B_2^p) B_3^p + (B_3^p - B_2^p) B_1^p]} \\ \sigma'_{13} &= \frac{\sqrt{2}}{8} \frac{(B_2^p - B_1^p) \left[\frac{\Delta R_4}{R_4} - \frac{\Delta R_2}{R_2} \right] - (B_2^n - B_1^n) \left[\frac{\Delta R_8}{R_8} - \frac{\Delta R_6}{R_6} \right]}{(B_2^p - B_1^p) B_3^p + (B_1^p - B_2^p) B_3^p + (B_3^p - B_2^p) B_1^p} \\ \sigma'_{23} &= \frac{\sqrt{2}}{8} \frac{-(B_2^p - B_1^p) \left[\frac{\Delta R_1}{R_1} - \frac{\Delta R_3}{R_3} \right] + (B_2^n - B_1^n) \left[\frac{\Delta R_5}{R_5} - \frac{\Delta R_7}{R_7} \right]}{(B_2^p - B_1^p) B_3^p + (B_1^p - B_2^p) B_3^p + (B_3^p - B_2^p) B_1^p} \\ \sigma'_{12} &= \frac{-(B_3^p - B_2^p) \left[\frac{\Delta R_4}{R_4} - \frac{\Delta R_2}{R_2} \right] + (B_3^n - B_2^n) \left[\frac{\Delta R_8}{R_8} - \frac{\Delta R_6}{R_6} \right]}{2[(B_2^p - B_1^p) B_3^p + (B_1^p - B_2^p) B_3^p + (B_3^p - B_2^p) B_1^p]} \end{aligned} \quad (1)$$

The Piezoresistive coefficients B_1 , B_2 , B_3 in eq. (1) were obtained using four-point bending, wafer level, and hydrostatic calibration methods. The average experimentally measured values are tabulated in Table 1. Further details on the calibration tests can be found in reference [6].

Piezoresistive Coefficients BMW-2 Test Chip (TPa^{-1})					
B_1^p	B_2^p	B_3^p	B_1^n	B_2^n	B_3^n
495	-122	-411	-220	216	36.8

Table 1

Packaging Studies

The BMW-2 stress test chips used in this study had dimensions of 400 x 400 x 20 mils or 10.2 x 10.2 x .5 mm (2 x 2 array of the die schematic shown in Figure 2). FR-4 printed circuit board (PCB) test vehicles were prepared with dimensions of 12.7 cm x 10.74 cm x 1.1 mm, and with one central die bond site. The test die were bonded to the FR-4 substrates using a silver-filled epoxy die attachment adhesive (Ablestik Ablebond 84-1LMI). Thermosonically bonded gold wires were then used to provide the interconnections from the die bond pads to the metal traces on the PCB's. Finally, the test chips were encapsulated using a "glob-top" epoxy coating (Dexter Hysol FP4651). A total of 24 specimens were prepared. The liquid encapsulant applied to the samples was then cured using either convection or VFM cure processes (12 samples were cured with each of the two methods). A schematic of the COB test specimen geometry is illustrated in Figure 4.

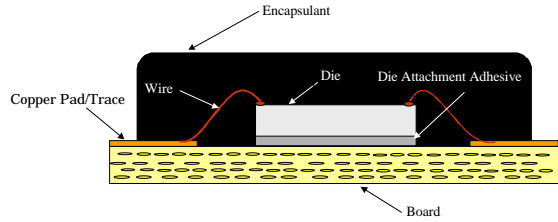


Figure 4 – Test Specimen Schematic

Although there are 20 accessible rosette sites on the 400 x 400 mil BMW-2 test die, only twelve were utilized in this study due to line width and routing limitations on the PCB. The copper traces on the PCB were routed to the edge of the board, and a standard edge connector was used to provide electrical connection of the samples to a data acquisition system. Figure 5 shows the selected rosette sites for stress measurement.

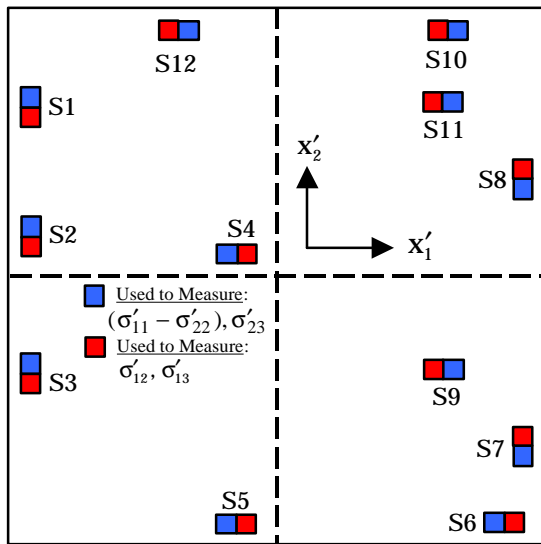


Figure 5 - Sensor Rosette Locations (400 x 400 mil Test Chip)

Before packaging, the initial room temperature resistances of all of the sensors were recorded when the chips were in wafer form using an automated probe station. The characterized test die were then diced from the wafers and bonded to the PCB's. After die attachment and wire bonding, the sensor resistances were again measured. Finally, the liquid encapsulant materials were applied and the samples were cured with the two types of ovens.

The chips were encapsulated using a dam (Dexter Hysol FP4451) and fill (Dexter Hysol FP4651) approach. A Camalot 3600 Dispenser with a 680 PDP positive displacement pump was used for dispensing the materials. The under-board heating

stage was set to 70 °C, and a spiral pattern was used to dispense the fill material.

For the specimens processed using a conventional convection cure, a Blue M oven was used. The convection cure profile was 2 hours at 110°C, followed by 3 hours at 165°C (5 hours total). After removal from the cure oven, the samples were cooled to a normal room temperature environment of 23 °C. Transient sensor resistances were monitored during the entire encapsulant cure process, and the post packaging room temperature resistances of the sensors were recorded.

For the specimens processed using variable frequency microwave curing, a MicroCure 5100 in-line system manufactured by Lambda Technologies was utilized. The cure profile as measured by IR pyrometry is shown in Figure 6. This profile consisted of 5 minutes at 110 °C, 5 minutes at 120 °C, 5 minutes at 130 °C, and 20 minutes at 165 °C (35 minutes total). An attempt was made to monitor the sensor resistances (stress) during the cure process. However, interference of electromagnetic energy with the measurement signals resulted in too much electrical noise for valid measurements. Thus, for the VFM cured specimens, only the post packaging room temperature stresses after cure cool down will be reported.

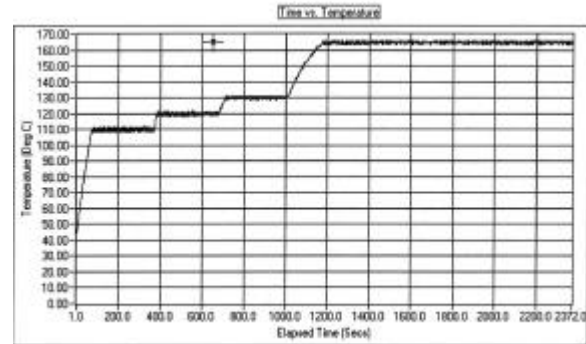


Figure 6 - VFM Curing Profile

After curing and cool down, stress variations in the final packaged die were measured as a function of temperature from -40 °C to +140 °C. Also, the 12 samples from each curing method were divided into two groups of 6, and reliability tests were performed. The first group of samples was subjected to thermal cycling between -40 °C and +125 °C. The second group was exposed to high humidity storage at 85% RH and 85 °C. In each case, changes in the die stress levels were monitored for samples from each curing method to detect delaminations due to thermal cycling to study the impact of moisture absorption

Stresses Due to Die Attachment

After the test chips were bonded to the FR-4 substrates, the die attachment adhesive was convection cured for 60 minutes at 150 °C per vendor instructions. The specimen assemblies were then cooled to room temperature and the thermosonic gold wire bonding was performed to interconnect the perimeter bond pads on the die to the substrate traces. Sensor resistances were recorded, and the die surface stresses induced by the die attachment process were calculated using these measurements and the resistance data recorded while the die were still in wafer form. At the die attach cure temperature, the adhesive is fairly relaxed/uncured and the die is nearly stress free. When the assembly is cooled down to room temperature, thermal stresses are generated in the die due to the differential shrinkages resulting from the differences in the coefficients of expansion of the die ($\alpha = 2.3 \times 10^{-6} \text{ 1/}^\circ\text{C}$), the die attachment adhesive ($\alpha = 55 \times 10^{-6} \text{ 1/}^\circ\text{C}$), and the FR-4 substrate ($\alpha = 15 \times 10^{-6} \text{ 1/}^\circ\text{C}$).

The measured values of the in-plane shear stress σ'_{12} and the in-plane normal stress difference ($\sigma'_{11} - \sigma'_{22}$) are shown in Figure 7. Each indicated value is the average of data taken from the entire set of 24 specimens. The magnitudes are universally small when compared to the stresses typically induced by topside encapsulation, where the sensor surface is contacted directly by a material of drastically different CTE. The signs of the measured normal stress difference values are in contrast to those presented in earlier work of the authors [8]. This was due to the relatively thin substrate used in this study. The average measured magnitudes of the out-of-plane shear stresses σ'_{13} and σ'_{23} were typically less than 1 MPa, a level that approaches the resolution limit of the experimental method. Note that these shear stresses are theoretically zero at this point in the packaging process, due to the fact that the die surface is still free of shear tractions.

Stress Variation During Encapsulant Cure

As mentioned previously, transient sensor resistances were monitored during the entire encapsulant cure process for the specimens cured in the convection oven. Typical data are illustrated in Figure 8, where the variation of the in-plane shear stress with time is shown at site 10 (location S10 in Figure 5) on one of the encapsulated test die. At time $t = 0$, the board had just been removed off of the hot plate after dispensing of the encapsulant, and inserted into the edge connector socket to initiate data collection. The sample was inserted into the

convection oven at approximately $t = 400$ sec for the gel portion of the encapsulant cure cycle. Between $t = 400$ sec and $t = 2000$ sec, the sample increased in temperature and eventually reached the gel temperature of 110 °C. The sample then remained at this temperature for 2 hours. At approximately $t = 10000$, the oven temperature was increased to 165 °C for the second portion of the encapsulant cure cycle. Upon completion of the 3 hours hold at 165 °C, the board was removed from the oven and allowed to cool in a room temperature environment.

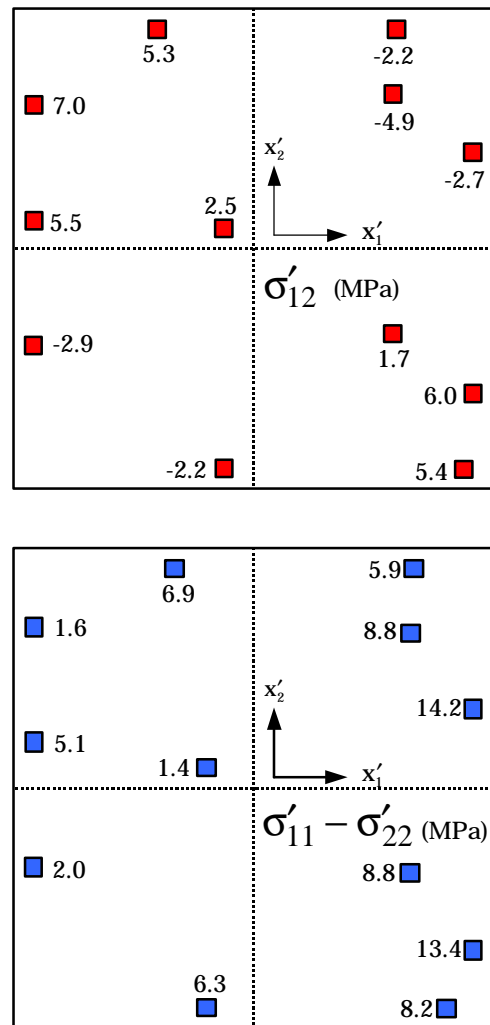


Figure 7 - Measured Stresses after Die Attachment

As seen in Figure 8, the majority of the final stress in the die was developed during this cool down period, where the encapsulant is fully hardened and can provide a significant stiffness to stress the low CTE silicon die material. A more complete discussion of the

die stress variation during the convection cure cycle has been given by the authors in reference [8].

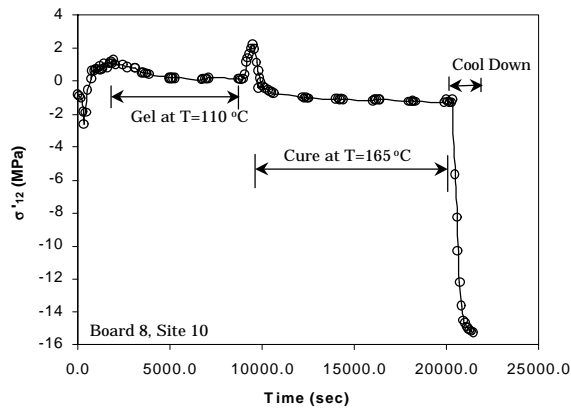


Figure 8 – Stress Variation During Convection Curing

Stresses After Encapsulation

The final stresses resulting after the encapsulant cure cycle and COB package cooling were calculated from the original (wafer level) and final (packaged) die sensor resistances, and eqs. (1). Since both of these measurements and the calibration of the piezoresistive coefficients were done at room temperature (23 °C), any unexpected thermal errors will be minimized. Figure 9 contains the measured data for the in-plane shear stress σ'_{12} , the in-plane normal stress difference ($\sigma'_{11} - \sigma'_{22}$), and the out-of-plane shear stresses σ'_{13} and σ'_{23} respectively. At every rosette site in each plot, results are given for both the convection cure and VFM cure processes. Each indicated value is the average of data taken from the 12 specimens used for each cure process.

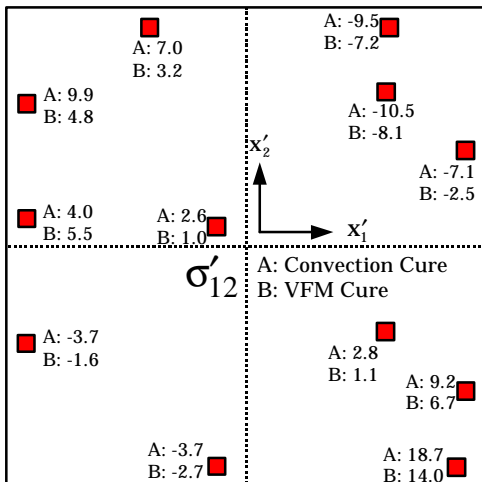
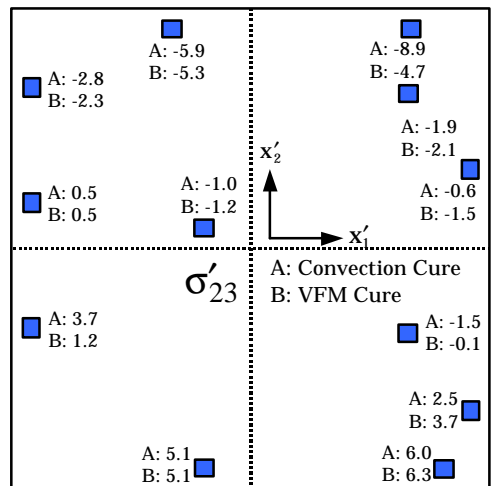
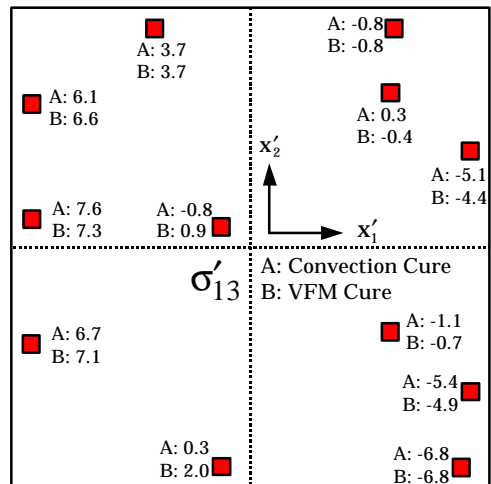
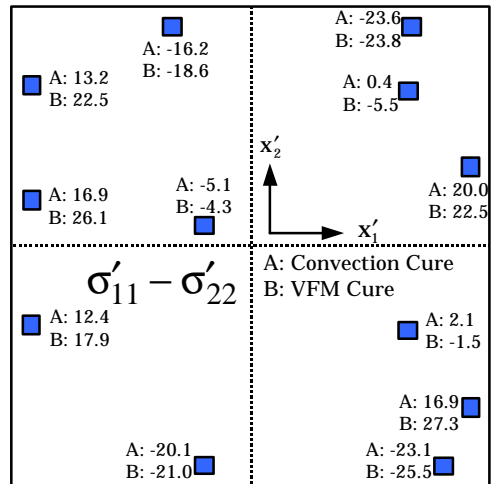


Figure 9 – Die Stresses After Encapsulation

No significant differences in the die stresses caused by convection and variable frequency microwave curing were observed. This is especially true for the out-of-plane shear stresses. For the in-plane shear stress, the stress magnitudes measured for convection cured specimens were slightly higher than those for VFM cured specimens (maximum stresses differed by 14%). However, the opposite trend was observed for the in-plane normal stress difference (maximum stresses differed by 25%). The out-of-plane shear stress magnitudes are relatively small for both curing processes when compared to the magnitudes of the in-plane stress components.

To further illustrate the nature of the stresses induced by encapsulation, two COB specimens (one from each type of cure process) were subjected to slow temperature change from $-40\text{ }^{\circ}\text{C}$ to $+140\text{ }^{\circ}\text{C}$. Resistance values were monitored continuously, and the stresses were extracted as a function of temperature. When using eqs. (1), it was assumed that the piezoresistive coefficients were approximately independent of temperature. Typical in-plane shear stress and in-plane normal stress difference data are shown in Figures 10 and 11, respectively. In all cases, raising the temperature from room temperature decreases the magnitude of the stress component. As the temperature approaches $165\text{ }^{\circ}\text{C}$ (the final cure temperature of the liquid encapsulant in both processes), the stresses approach zero. Likewise, at lower temperatures the stress levels are increased. This is because the material expansion mismatch becomes worse due to the larger temperature change from the “relaxed” configuration of the package materials at approximately $165\text{ }^{\circ}\text{C}$. Similar trends were found in the stress variations with temperature for both the convection and VFM curing processes.

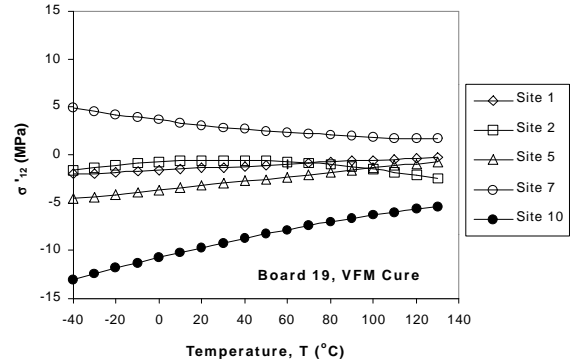
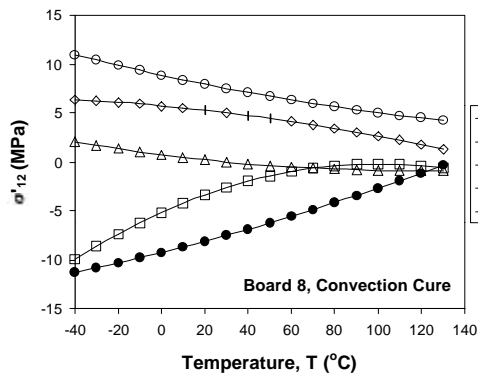


Figure 10 - Variation of Final Packaged Die Stress with Temperature (σ'_{12})

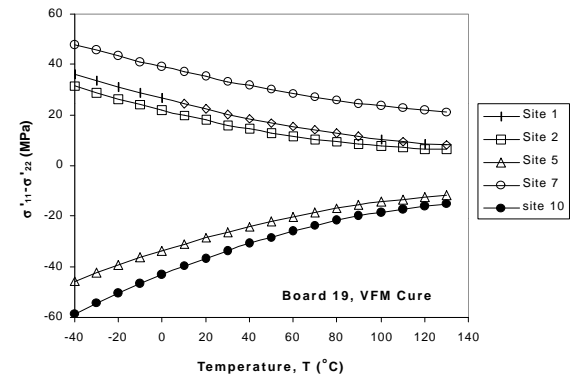
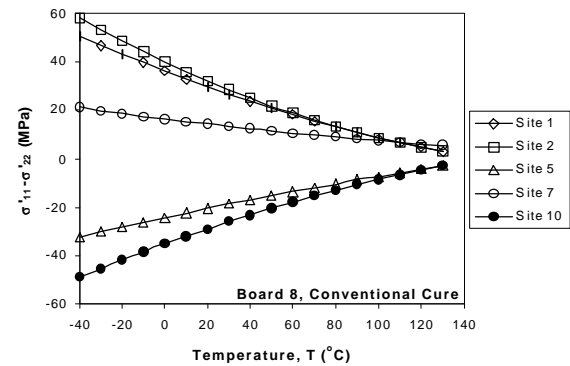


Figure 11 - Variation of Final Packaged Die Stress with Temperature ($\sigma'_{11} - \sigma'_{22}$)

Stresses Due to Thermal Cycling and Moisture Absorption

After performing the measurements discussed above, the samples from each curing method were divided into two groups, and reliability tests were carried out to evaluate the capability of the COB

samples to survive a variety of severe environments. Specimens from the first group were subjected to thermal cycling between $-40\text{ }^{\circ}\text{C}$ and $+125\text{ }^{\circ}\text{C}$. A total of 900 thermal cycles have been finished to date, and further cycling is underway. The second group was exposed to high humidity storage at 85% RH and $85\text{ }^{\circ}\text{C}$ for 168 hours. In each case, changes in the die stress levels were monitored for samples from each curing method in order to detect delaminations and other failures, and to study the impact of moisture absorption. A brief discussion of the observed results is now presented.

Site #	Cure	Number of Thermal Cycles			
		0	100	200	900
S1	A	11.3	9.8	9.2	6.9
	B	6.4	6.6	6.7	3.7
S2	A	4.3	3.5	3.1	1.5
	B	5.3	5.7	5.9	4.8
S3	A	-3.6	-4.3	-4.6	-4.2
	B	-1.5	-0.8	0.2	1.1
S4	A	-1.1	1.1	1.6	1.5
	B	-0.4	1.1	2.2	2.1
S5	A	-5.7	-4.7	-4.4	-2.4
	B	-3.4	-0.4	1.0	0.3
S6	A	17.8	19.9	18.2	12.7
	B	15.2	17.4	16.7	14.3
S7	A	9.6	8.5	8.2	7.0
	B	8.8	8.1	7.3	7.1
S8	A	-8.8	-9.1	-9.4	-8.2
	B	-3.4	-2.3	-1.2	-0.2
S9	A	4.5	1.5	1.7	0.9
	B	2.0	0.8	0.7	0.4
S10	A	-10.2	-9.6	-9.5	-8.0
	B	-6.3	-5.2	-4.7	-3.4
S11	A	-7.8	-6.2	-6.8	-6.6
	B	-7.8	-6.1	-5.8	-4.8
S12	A	7.0	5.6	5.5	4.3
	B	4.7	4.6	4.7	3.7

(A: Convection Cure, B: VFM Cure, Stresses in MPa)

Table 2(a) – Stress Variation Due to Thermal Cycling (σ'_{12})

Site #	Cure	Number of Thermal Cycles			
		0	100	200	900
S1	A	16.1	15.7	16.9	17.3
	B	22.8	23.4	22.9	22.6
S2	A	13.4	13.5	14.6	13.0
	B	28.1	30.9	32.4	29.1
S3	A	11.8	11.1	11.5	8.6
	B	17.8	21.3	20.1	21.2
S4	A	-3.0	-5.1	-4.9	-6.1
	B	-3.3	-3.8	-6.8	-7.7
S5	A	-26.0	-27.2	-32.6	-35.0
	B	-22.3	-26.1	-27.0	-25.4
S6	A	-25.6	-25.8	-27.3	-27.0
	B	-25.0	-25.2	-26.6	-26.2
S7	A	10.2	12.0	10.8	5.6
	B	24.8	23.7	23.2	20.8
S8	A	15.1	12.2	12.3	14.8
	B	23.7	24.0	25.1	22.2
S9	A	0.5	1.1	0.8	0.3
	B	3.2	2.8	2.1	1.7
S10	A	-19.3	-14.5	-12.9	-14.5
	B	-23.3	-24.3	-27.2	-24.8
S11	A	-1.3	-2.0	-5.1	-3.9
	B	-5.4	-5.8	-4.3	-3.6
S12	A	-24.1	-22.5	-23.3	-21.5
	B	-17.7	-21.2	-23.2	-23.3

(A: Convection Cure, B: VFM Cure, Stresses in MPa)

Table 2(b) – Stress Variation Due to Thermal Cycling ($\sigma'_{11} - \sigma'_{22}$)

The thermal cycling tests have been performed in three stages (100, 100, 700 cycles) for a total of 900 cycles. After each round of cycling, the samples were taken out of the oven and the resistances of all the sensors on the test die were recorded at room temperature. The die stresses after each thermal cycling iteration were then extracted by using eqs. (1). Tables 2(a,b) illustrate the stress variations during the thermal cycling tests for the in-plane shear stress and in-plane normal stress difference. The stress changes at various points in the cycling show similar trends for the two curing processes. Small stress increases were observed in the in-plane normal stress difference ($\sigma'_{11} - \sigma'_{22}$), demonstrating that further curing of the encapsulant could be occurring during the early thermal cycling. Conversely, a small amount of stress decrease/relief is illustrated in the in-plane shear stress (σ'_{12}) data for both cure methods. This indicates potential creep of the epoxy material and/or possible initiation of delaminations or encapsulant cracking. In any case, the stress variations were small over the 900 cycles for both curing methods. Also, the results illustrate similar trends for the stress variations in the samples cured with convection and VFM systems. Both curing methods yielded specimens that were reliable to 900 cycles, and no failures were observed. Further thermal cycling of the sample is currently in progress.

Room temperature stress results before and after high humidity storage (for 168 hours at 85% RH and $85\text{ }^{\circ}\text{C}$) are shown in Tables 3(a,b). The trends shown in the stress variations were found to be the same as in the thermal cycling tests, and both curing methods yielded reliable samples.

Site #	Cure	Before Testing	After Testing
S1	A	10.3	6.5
	B	3.0	4.0
S2	A	4.1	2.4
	B	5.3	3.3
S3	A	-4.1	-3.7
	B	-2.2	-0.1
S4	A	3.5	1.2
	B	0.1	0.0
S5	A	-2.0	-0.5
	B	-2.0	0.0
S6	A	19.0	15.6
	B	10.8	10.7
S7	A	8.6	5.6
	B	5.4	5.1
S8	A	-4.1	-2.3
	B	-0.9	-0.9
S9	A	0.1	1.2
	B	1.2	0.6
S10	A	-9.9	-6.3
	B	-7.3	-5.2
S11	A	-13.3	-9.4
	B	-8.4	-5.7
S12	A	6.2	3.8
	B	2.0	3.2

(A: Convection Cure, B: VFM Cure, Stresses in MPa)

Table 3(a) – Stress Variation Due to High Humidity Storage (σ'_{12})

Site #	Cure	Before Testing	After Testing
S1	A	11.1	14.0
	B	22.2	23.9
S2	A	21.0	17.4
	B	25.6	35.1
S3	A	13.6	15.1
	B	18.1	26.8
S4	A	-6.9	-3.4
	B	-2.8	-0.3
S5	A	-17.1	-14.6
	B	-16.6	-21.5
S6	A	-19.0	-16.1
	B	-26.2	-22.8
S7	A	21.9	20.7
	B	26.9	31.0
S8	A	28.1	28.5
	B	23.0	28.8
S9	A	4.2	4.1
	B	3.1	5.1
S10	A	-29.3	-12.4
	B	-23.3	-24.6
S11	A	1.2	3.6
	B	-5.7	-3.2
S12	A	-5.2	-4.8
	B	-18.6	-22.6

(A: Convection Cure, B: VFM Cure, Stresses in MPa)

Table 3(b) – Stress Variation Due to High Humidity Storage ($\sigma'_{11} - \sigma'_{22}$)

Substrate Warpage Measurements

A comparison of the stresses introduced at the FR-4 board level during encapsulant cure by convection and VFM processes was conducted using PCB warpage measurements. The FR-4 laminate material was cut into 100 mm x 25 mm x .55 mm samples. An Asymtek Century Dispenser was used to dispense 450 mg of Dexter Hysol FP4451 to form a 90 mm x 20 mm dam. Dexter Hysol FP4651 encapsulant (1500 mg) was dispensed to fill the dam area. The hot plate was at 80°C during the dispensing process. A schematic of the warpage test sample is illustrated in Figure 12.

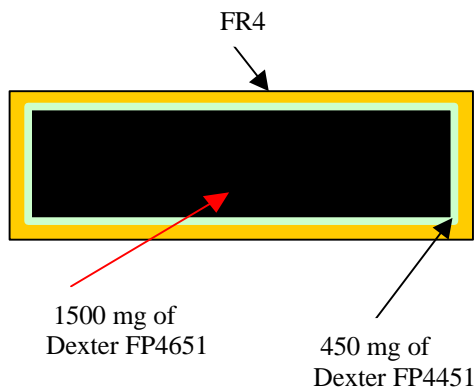


Figure 12 - Illustration of the Warpage Study Test Coupon.

A total of 16 samples were prepared. Eight were cured in the convection oven at 110 °C for 2 hours followed by 165 °C for 3 hours. The other eight were cured using VFM with 5 minutes hold at 110 °C, 5 minutes at 120 °C, 5 minutes at 130 °C, and 20 minutes 165 °C degrees.

The maximum warpage displacements of the samples were measured using a Mitutoyo Absolute Electronic Indicator. The substrate was placed on a smooth surface, and the linear position plunger of the indicator was placed on one end of the substrate and the electronic indicator was reset with this position as the origin. The other end was then depressed on the smooth surface and the digital reading noted for each of the substrates. The setup is shown in Figure 13, and the measurements for the specimens cured with convection and VFM curing are shown in Table 4. The warpage displacements for the assemblies with VFM cured encapsulants were less than those for convection cured samples. The average maximum displacement for convection curing was 4.75 mm, whereas it was 3.87 mm for VFM curing, showing an 18% improvement with the VFM process.

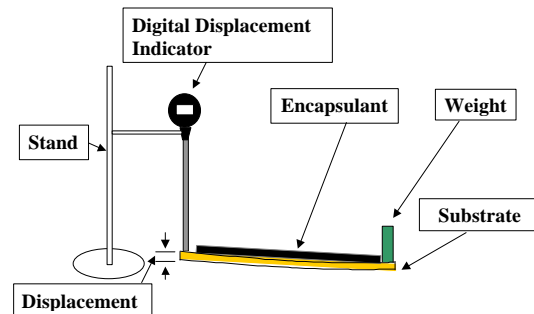


Figure 13 - Setup for Displacement Measurements

Specimen Number	Displacement (mm)	
	Convection Curing	VFM Curing
1	4.2	2.74
2	5.71	4.16
3	5.13	3.39
4	4.87	3.79
5	4.06	3.87
6	5.20	4.35
7	3.85	5.04
8	4.98	3.65
Average	4.75	3.87
Std. Dev.	0.65	0.68

Table 4 - Comparison of Warpage Displacements

Summary and Conclusions

Die surface stresses in COB packages were measured for a commercial encapsulant cured with both convection and variable frequency microwave curing. The utilized stress test chips contained an array of optimized sensor rosettes that are capable of evaluating the complete stress at points on the surface of the die. Stresses were monitored in-situ during the convection cure cycle. However, microwave interference with the measurement signals did not permit in-situ monitoring for the VFM cure. A comparison was made between the room temperature stresses found with each method of curing. Differences from 0-25% were observed in the maximum values of the in-plane die stresses caused by convection and VFM microwave curing. Differences in the out-of-plane shear stresses produced with each cure process were minimal.

After cure, the samples from each curing method were divided into two groups, and reliability tests were performed. The first group of samples was subjected to thermal cycling over the range of $-40\text{ }^{\circ}\text{C}$ and $+125\text{ }^{\circ}\text{C}$. The second group was exposed to high humidity storage at 85% RH and $85\text{ }^{\circ}\text{C}$. In both cases, the stress variations were found to be small over the entire duration of the reliability testing. Also, the results illustrated similar trends for the stress variations in the samples cured with convection and VFM systems. Both curing methods yielded specimens that were reliable, and no failures were observed.

Finally, a comparison of the stresses introduced at the FR-4 board level for each curing method was made through substrate warpage measurements. The warpage displacements for the VFM cured assemblies averaged 18% less than those for convection cured samples. Overall, VFM curing was found to offer similar die stress levels and reliability, reduction in substrate warpage, and greatly reduced cure times when compared to conventional convection curing.

References

- [1] Z. Fathi, D. Tucker, I. Ahmad, E. Yeager, M. Konarski, L. Crane and J. Heaton, "Innovative Curing of High Reliability Advanced Polymeric Encapsulants," *Proceedings of NEPCON West*, 1998.
- [2] B. Anderson, I. Ahmad, D. Tucker, S. Goldstein, Z. Fathi, A. Ramamoorthy, S. Pal, and P. Mead, "Rapid Processing and Properties Evaluation of Flip Chip Underfills," *Proceedings of NEPCON West*, 1998.
- [3] Sweet, J. N., "Die Stress Measurement Using Piezoresistive Stress Sensors," in *Thermal Stress and Strain in Microelectronics Packaging*, Edited by J. Lau, Von Nostrand Reinhold, 1993.
- [4] Bittle, D. A., Suhling, J. C., Beaty, R. E., Jaeger, R. C. and Johnson, R. W., "Piezoresistive Stress Sensors for Structural Analysis of Electronic Packages," *Journal of Electronic Packaging*, Vol. 113(3), pp. 203-215, 1991.
- [5] Cordes, R. A., Suhling, J. C., Kang, Y. and Jaeger, R. C., "Optimal Temperature Compensated Piezoresistive Stress Sensor Rosettes," in the *Proceedings of the Symposium on Applications of Experimental Mechanics to Electronic Packaging*, American Society of Mechanical Engineers, EEP-Vol. 13, pp. 109-116, 1995.
- [6] Suhling, J. C., Jaeger, R. C., Lin, S. T., Mian, A. K. M., Cordes, R. A. and Wilamowski, B. M., "Design and Calibration of Optimized (111) Silicon Stress Sensing Test Chips," *Proceedings of INTERpack '97*, pp. 1723-1729, Kohala, HI, June 15-19, 1997.
- [7] Y. Zou, J. C. Suhling, R. C. Jaeger and H. Ali, "Three-Dimensional Die Surface Stress Measurements in Delaminated and Non-Delaminated Plastic Packaging," *Proceedings of the 48th Electronic Components and Technology Conference*, pp. 1223-1234, Seattle, WA, May 25-28, 1998.
- [8] Zou, Y., Suhling, J. C., Jaeger, R. C., and Johnson, R. W., "Complete Stress Measurements in Chip On Board Packages," *Proceedings of MCM'98*, pp. 405-415, Denver, CO, April 15-17, 1998.